



## $\gamma$ -Alumina Vanadate ( $\text{AlV}_2\text{O}_7$ ) Nanoparticles: Synthesis and Characterization

**RANJANA CHOUDHARY AHIRWAR<sup>1\*</sup> and RAJESH BABU AHIRWAR<sup>2</sup>**

<sup>\*1,2</sup>IPS Academy, Institute of Engineering & Science Indore Madhya Pradesh 452012, India.

\*Corresponding author E-mail: ranjna.rajesh@gmail.com

<http://dx.doi.org/10.13005/ojc/400213>

(Received: March 08, 2024; Accepted: April 29, 2024)

### ABSTRACT

Solution combustion Method for synthesis of alumina nanoparticles in a microwave oven represents a well-established technique for the fabrication of bimetallic metal oxide nanomaterials. In this process, citric acid functions as a pivotal fuel, facilitating the combustion of single-phase oxide materials and enabling the synthesis of multiphase nanomaterials. Utilizing self-propagating combustion methods with citric acid as the fuel source, nanoscale Alumina vanadate ( $\text{AlV}_2\text{O}_7$ ) materials can be successfully synthesized. The synthesis procedure involves the ignition of Aluminum oxide ( $\text{AlO}_2$ ) and ammonium meta-vanadate ( $\text{NH}_4(\text{VO}_3)$ ) in an open environment, allowing complete combustion to occur within approximately 15 min in a microwave setting. The precursor concentrations used 13.31 g/50 mL for Aluminum oxide and 0.7291 g/50 mL for ammonium meta-vanadate. Heating parameters included a microwave power of 2.45GHZ 800 watts and a reaction time of 15 minutes. Subsequent research endeavors have focused on investigating the adsorption behavior of lead and mercury ions onto the resultant sample. Due to the impressive adsorption active sites that are present on the sample, this sample exhibits significant adsorption. The produced metal oxide sample behaves well as adsorbents for heavy metal ions, according to an adsorption research., and their potential applications can be use as Catalysis, sensing, Energy Storage, Environmental Remediation. The structural characteristics of the as-prepared  $\text{AlV}_2\text{O}_7$  and the adsorbed sample were meticulously examined using powder X-ray diffraction (XRD) analysis. Morphological analysis of the freshly synthesized  $\text{AlV}_2\text{O}_7$  and the adsorbed sample material was conducted using scanning electron microscopy (SEM) and Transmission Electronic Microscopy (TEM). FTIR Analysis was also employed to characterize the functional groups present the peak  $3800\text{ cm}^{-1}$  corresponds to the water of absorption's vibration frequency at  $1089\text{ cm}^{-1}$  are assigned to the V=O stretching mode. RAMAN ( $125.1$ ,  $213.6$  and  $307.2\text{ cm}^{-1}$  is assigned to  $\text{AlO}_2$ ) and The band appeared at  $702\text{ cm}^{-1}$  in the Raman spectrum can be ascribed to stretching vibration of short V=O bond. Furthermore, a comprehensive study was carried out to evaluate the adsorption efficacy of heavy metal ions onto the  $\text{AlV}_2\text{O}_7$  sample at ambient temperature (400-600 ).

**Keywords:** Alumina Oxide, Ammonium Meta Vanadate, Citric acid, XRD, SEM, TEM.

### INTRODUCTION

The synthesis of nanomaterials through solution combustion processes has gained significant

attention in recent years due to its efficiency and versatility. Particularly, the use of microwave-assisted solution combustion offers a rapid and effective means of producing bimetallic metal oxide



nanomaterials with tailored properties. One of the key components in this synthesis method is citric acid, which serves as a fuel during the combustion process, enabling the formation of multiphase nanomaterials from Single-phase oxide precursors. In this context, the synthesis of nanoscale Alumina vanadate ( $\text{AlV}_2\text{O}_7$ ) materials using self-propagating combustion techniques with citric acid as the fuel has emerged as an area of interest. The combustion process involves igniting Aluminum oxide ( $\text{AlO}_2$ ) and ammonium meta-vanadate ( $\text{NH}_4(\text{VO}_3)$ ) precursors in an open environment, allowing them to undergo complete combustion within a short duration, typically around 15 min, under microwave irradiation. The resulting  $\text{AlV}_2\text{O}_7$  nanomaterials hold potential for various applications, particularly in environmental remediation, such as the adsorption of heavy metal ions like lead and mercury. Understanding the structural, morphological, and chemical properties of these nanomaterials is crucial for optimizing their performance in such applications.

This paper aims to investigate the synthesis process of  $\text{AlV}_2\text{O}_7$  nanomaterials via solution combustion in a microwave oven, as well as to explore their potential for heavy metal ion adsorption. The structural characterization of the synthesized  $\text{AlV}_2\text{O}_7$  and the adsorption behavior of heavy metal ions onto the nanomaterials will be thoroughly examined using advanced analytical techniques such as powder X-ray diffraction (XRD), scanning electron microscopy (SEM), Transmission Electronic Microscopy (TEM), and Fourier Transform Infrared (FTIR) spectroscopy.

By elucidating the synthesis mechanism and characterizing the properties of  $\text{AlV}_2\text{O}_7$  nanomaterials, this research aims to contribute to the development of efficient and sustainable nanomaterials for environmental applications.

In this context, the term "fuel" refers to the role of citric acid in facilitating the synthesis of  $\text{AlV}_2\text{O}_7$ . Citric acid acts as a fuel or a reducing agent, supplying carbon atoms and undergoing combustion-like reactions during the synthesis process. It undergoes thermal decomposition at elevated temperatures, leading to the release of reducing gases, such as carbon monoxide ( $\text{CO}$ ) and carbon dioxide ( $\text{CO}_2$ ). These reducing gases help create an oxygen-deficient atmosphere necessary for the formation of  $\text{AlV}_2\text{O}_7$ .

**Complexing agent:** Citric acid also acts as a complexing agent, forming stable complexes with the metal ions present in the Aluminum and vanadium salts. It binds to these metal ions, preventing their precipitation or agglomeration and keeping them in solution. This complexation process helps in controlling the reaction kinetics, ensuring uniform distribution of the metal ions, and promoting the formation of the desired compound,  $\text{AlV}_2\text{O}_7$ .

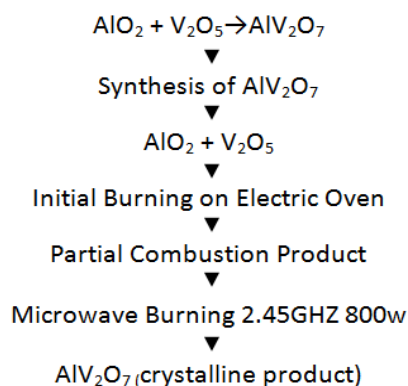
### Material and synthesis preparation

The solution combustion process was used to make Alumina vanadate<sup>13-15</sup>. The Alumina and vanadium salts, as well as citric acid, are used in this process.

### Composition of salt

1.  $\text{AlO}_2 = 13.31$  g
2.  $\text{NH}_4(\text{VO}_3) = 0.7291$  g
3. Citric acid = 27.91 g

To make slurry, combine all of the ingredients in a small amount of water. Heat the slurry until it forms a gel. In order to create Aluminum vanadate ( $\text{AlV}_2\text{O}_7$ ) nanomaterials, the resulting mixture was put into a crucible and burned on an electric oven to ensure that all of the vapors were completely expelled. It is then moved into a microwave oven to finish the calcinations process. The sample is calcined in a 2.45 GHz microwave oven. 800 watts are used at a frequency of once every 15 minutes. The reaction's approximate temperature while burning may be close to 400°C. The reaction mixture burns, producing a solid, crystalline byproduct of Aluminum vanadate. The material was then crushed and transferred to a muffle furnace for calcinations at 600 for 5 to 6 hours. The finished product is a yellow-green substance that has been ground into a fine powder<sup>15</sup>.



Scheme 1. Synthesis of Aluminum Vanadate

### Adsorption study

In double-distilled water, a lead acetate solution (200 ppm) is created. A single column containing 0.5 g of the prepared Aluminum vanadate sample and supported by cotton wool is filled with a known volume (25 mL) of the solution. It takes 24 h for this column to absorb everything. The reaction mixture solution is removed and put through an atomic absorption analysis (AAS). To determine the lead ion adsorption on the Aluminum vanadate adsorbent, the adsorbed sample is dried at room temperature and is subjected to structural, morphological, and bonding characterization. On a sample of Aluminum vanadate, same research is done with mercury metal ions.

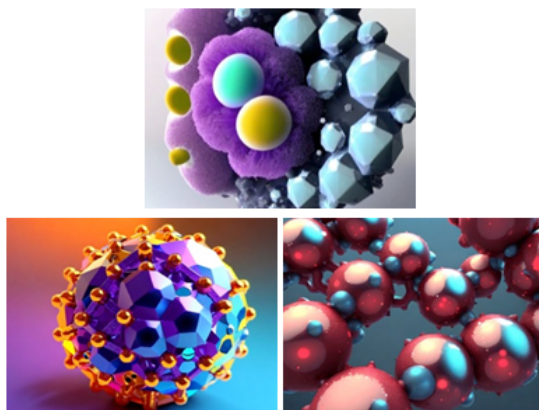


Fig. 1. Aluminum vanadate Nano-particle 3D Image

### Characterization

By employing an X' Pert Pro X-ray diffractometer and a Cu K source of radiation in a-2 configuration, the structures of zirconium vanadate as prepared were examined. JSM-6380 LA by JEOL Particle morphology is studied using a scanning electron microscope with energy dispersive which confirms the sample's metal content. The Technai-20 Philips transmission electron microscope is used to create TEM images. At 190 KeV, the transmission electron microscope was in operation.

## RESULTS AND DISCUSSION

### X-ray diffraction

The structural characteristics of the as-prepared  $\text{AlV}_2\text{O}_7$  and the adsorbed sample were meticulously examined using powder X-ray diffraction (XRD) analysis the steep peak formed around  $30.2^\circ$ , which corresponds to  $\text{AlO}_2$ 's tetragonal phase. With the use of Scherer's equation, the

particle's average size is calculated to be 25-30 nm. Calculated BET Surface Area ( $188.00 \text{ m}^2 \text{ g}$ ).

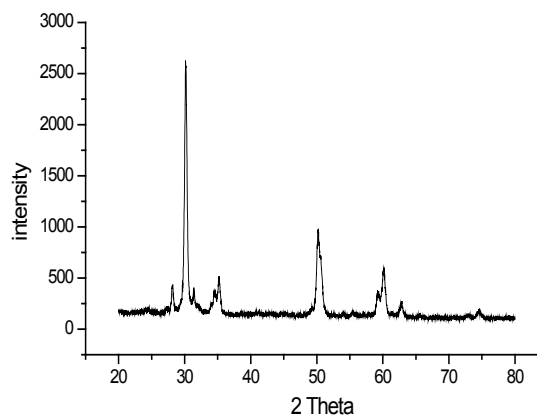


Fig. 2. XRD pattern of Aluminum vanadate

### Scanning Electron Microscopy

An as-prepared Aluminum vanadate sample is depicted in a SEM image in Fig. 3. The particles in this image are in the nanoscale, and the majority of them are spherical with a self-assembled compact shape. Additionally, due to crystalline nature, certain particles have irregular forms and self-assembled arrangements. (SEM Image with scale bar 200-500 nm) SEM image reveals that the agglomerated Spheroidal vanadium oxides particles were homogeneously deposited on the  $-\text{AlV}_2\text{O}_7$  support surface.

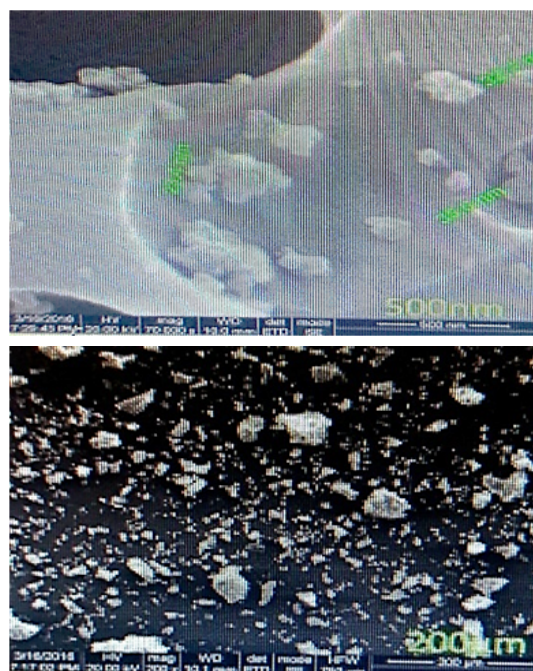


Fig. 3. SEM image of the  $\text{AlV}_2\text{O}_7$  sample

### Transmission Electronic Microscopy

The prepared Aluminum vanadate sample's TEM picture. The crystalline form of the sample is seen in the photograph along with small particles. The image shows particles with complexity development and dense structure. The nano range includes particles with an irregular form and a range of sizes (5-10 nm). Close aggregation with the compact is also seen in some areas, which may be a useful shape as an excellent adsorbent for metal ions.

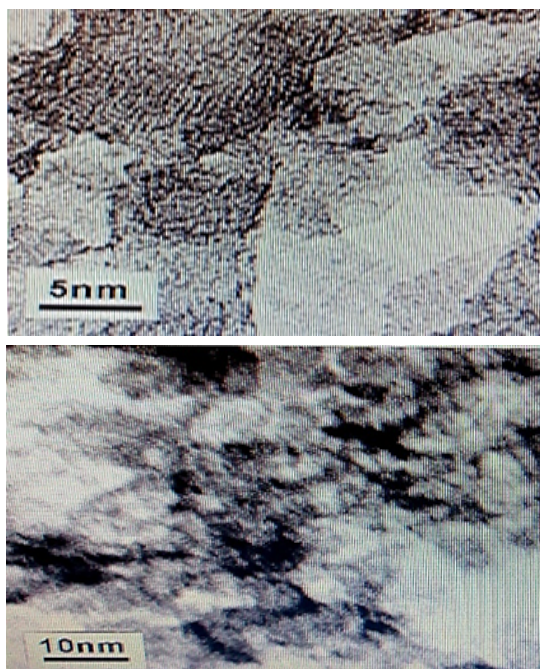


Fig. 4. TEM image of the  $\text{AlV}_2\text{O}_7$  sample

### FT-IR-RAMAN spectrum

The Aluminum vanadate sample's FT-IR spectrum is displayed in Fig. 5. The infrared study was used to determine the nature of the synthesized Aluminum vanadate sample and the metal-oxygen bonding. Metal oxides typically produce interatomic vibration-induced absorption bands approx  $1000 \text{ cm}^{-1}$  <sup>16-21</sup>. Due to the presence of various overtones, the peak  $3800 \text{ cm}^{-1}$  corresponds to the water of absorption's vibration frequency at  $1089 \text{ cm}^{-1}$ . Peaks below  $1000 \text{ cm}^{-1}$  that are in accordance with the sample's Metal-oxygen vibrational modes support the synthesis of Aluminum vanadate <sup>22</sup>.

The bands appeared at  $125.1$ ,  $213.6$  and  $307.2 \text{ cm}^{-1}$  is assigned to  $\text{AlO}_2$ . The low frequency bands appeared at  $125.1$ ,  $213.6$  are assigned to lattice vibrations. Bands appeared at  $524.2 \text{ cm}^{-1}$  can

be attributed to bending modes of water. The band appeared at  $702 \text{ cm}^{-1}$  in the Raman spectrum can be ascribed to stretching vibration of short  $\text{V}=\text{O}$  bond. A strong Raman band at  $674.2 \text{ cm}^{-1}$  is generally assigned to  $\text{V}=\text{O}$  stretching mode of bulk  $\text{V}_2\text{O}_7$  <sup>25</sup>. Weak intensity of this band in the present recording suggests low concentration of bulk  $\text{V}_2\text{O}_7$ .

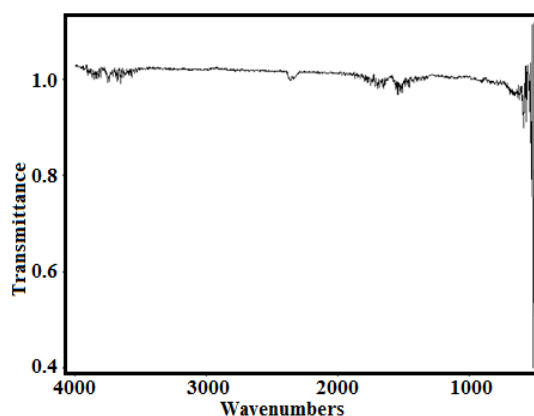


Fig. 5. FT-IR spectrum of the  $\text{AlV}_2\text{O}_7$  sample

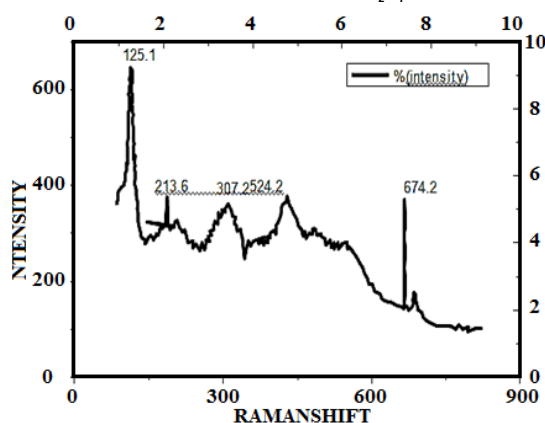


Fig. 6. RAMAN spectrum of the  $\text{AlV}_2\text{O}_7$  sample

### Adsorption study

Results of the AAS for fluid lead and mercury solutions and pure lead and mercury solutions are shown in Table 1 after adsorption. The data makes it evident that the loss of lead and mercury ions by adsorption on the Aluminum vanadate sample is confirmed by the decrease in the concentration of eluent lead and mercury solution compared to plain lead and mercury solution. Due to the impressive adsorption active sites that are present on the sample, this sample exhibits significant adsorption <sup>23</sup>. The produced metal oxide sample behaves well as adsorbents for heavy metal ions, according to an adsorption research.

**Table 1: AAS results of lead and mercury adsorption on the AlV<sub>2</sub>O<sub>7</sub> sample**

Sn. No	Concentration	Concentration of Pb <sup>2+</sup> solution (ppm Or mg/L)	Concentration of Hg <sup>2+</sup> solution (ppm or mg/L)
1	Initial concentration	200 mg/L	200 mg/L
2	Concentration After passing through AlV <sub>2</sub> O <sub>7</sub> sample	120 mg/L	130 mg/L

### CONCLUSION

The Aluminum vanadate sample is successfully synthesized through a combustion process using citric acid as fuel. Subsequent research endeavors have focused on investigating the adsorption behavior of lead and mercury ions onto the resultant sample. And Due to the impressive adsorption active sites that are present on the sample, this sample exhibits significant adsorption. The produced metal oxide sample behaves well as adsorbents for heavy metal ions, according to an adsorption research., and their potential applications can be use as Catalysis, sensing, Energy Storage,

Environmental Remediation. Through straight forward Various testing's I.e. XRD analysis (30.2°) RAMAN (125.1, 213.6 and 307.2 cm<sup>-1</sup> is assigned to AlO<sub>2</sub>) and The band appeared at 702 cm<sup>-1</sup> in the Raman spectrum can be ascribed to stretching vibration of short V=O bond. FT-IR (1038 cm<sup>-1</sup>) Peaks below 1000 cm<sup>-1</sup> that are in accordance with the sample's Metal-oxygen vibrational modes support the synthesis of Aluminum vanadate. SEM (200 nm-500 nm), TEM (5-10 nm). This solid-state process produced the phase development of an oxide sample. The produced sample functions well as an adsorbent for heavy metal ions, according to an adsorption investigation.

### ACKNOWLEDGEMENT

The authors are thankful to UGC-DAE-CSR (UGC-DAE Consortium for Scientific Research), Indore, India for XRD analysis. Dr. Hari Singh Gour Sagar Central University India for FT-IR Spectroscopy analysis.

### Conflict of Interests

The authors say they have no conflict interests.

### REFERENCES

- Brahma, S.; Liu, C.P.; Shivashankar, S.A. Microwave irradiation assisted, one pot synthesis of simple and complex metal oxide nanoparticles: a general approach., *Journal of Physics D: Applied Physics.*, **2017**, 50.
- Aivazoglou, E.; Metaxa, E.; Hristoforou, E. Microwave-assisted synthesis of iron oxide nanoparticles in biocompatible organic environment., *AIP Advances.*, **2017**, 8, <http://doi.org/10.1063/1.4994057>.
- Hamelian, M.; Varmira, K.; Veisi, H. Green synthesis and characterizations of gold nanoparticles using Thyme and survey cytotoxic effect, antibacterial and antioxidant potential., *Journal of Photochemistry and Photobiology B: Biology.*, **2018**, 184, 71-79, <https://doi.org/10.1016/j.jphotobiol.2018.05.016>.
- Rodrigues, B.S.; Branco, C.M.; Corio, P.; Souza, J.S. Controlling Bismuth Vanadate Morphology and Crystalline Structure through Optimization of Microwave-Assisted Synthesis Conditions., *Crystal Growth & Design.*, **2020**, 20, 3673-3685, <https://doi.org/10.1021/acs.cgd.9b01517>.
- Ceballos-Chuc, M.C.; Ramos-Castillo, C.M.; Alvarado-Gil, J.J.; Oskam, G.; Rodriguez-Gattorno, G. Influence of Brookite Impurities on the Raman Spectrum of TiO<sub>2</sub> Anatase Nanocrystals., *The Journal of Physical Chemistry C.*, **2018**, 122, 19921-19930, <https://doi.org/10.1021/acs.jpcc.8b04987>.
- Ashraf, H.; Anjum, T.; Riaz, S.; Naseem, S. Microwave-Assisted Green Synthesis and Characterization of Silver Nanoparticles Using Melia azedarach for the Management of Fusarium Wilt in Tomato., **2020**, 11, 12- 21, <https://doi.org/10.3389/fmicb.2020.00238>.
- Aritonang, H.F.; Koleangan, H.; Wuntu, A.D. Synthesis of silver nanoparticles using aqueous extract of medicinal plants' fresh land analysis of antimicrobial activity., *International Journal of Microbiology.*, **2019**, 2019, <https://doi.org/10.1155/2019/8642303>.
- Al-Haddad, J.; Alzaabi, F.; Pal, P.; Rambabu, K.; Banat, F. Green synthesis of bimetallic copper-silver nanoparticles and their application in catalytic and antibacterial activities., *Clean Technologies and Environmental Policy.*, **2020**, 22, 269-277, <https://doi.org/10.1007/s10098-019-01765-2>.

9. Ganiger, S.K.; Murugendrappa, M.V. Lab Scale Study on Humidity Sensing and D.C. Conductivity of Polypyrrole/Strontium Arsenate ( $\text{Sr}_3(\text{AsO}_4)_2$ ) Ceramic Composites., *Polymer Science, Series B*, **2018**, *60*, 395-404, <https://doi.org/10.1134/S1560090418030119>.
10. Bashir, A.; Malik, L.A.; Dar, G.N.; Pandith, A.H. Microwave-Assisted Hydrothermal Synthesis of Agglomerated Spherical Zirconium Phosphate for Removal of  $\text{Cs}^+$  and  $\text{Sr}^{2+}$  Ions from Aqueous System., *Applications of Ion Exchange Materials in the Environment*, **2019**, *65*, 95-108, [http://doi.org/10.1007/978-3-030-10430-6\\_5](http://doi.org/10.1007/978-3-030-10430-6_5)
11. Fierascu, I.; Fierascu, I.C.; Brazdis, R.I.; Baroi, A.M.; Fistos, T.; Fierascu, R.C. Phytosynthesized Metallic Nanoparticles-between Nanomedicine and Toxicology. A Brief Review of 2019 s Findings., *Materials*, **2020**, *13*, <https://doi.org/10.3390/ma13030574>.
12. Chand, K.; Cao, D.; Eldin Fouad, D.; Hussain Shah, A.; Qadeer Dayo, A.; Zh u, K.; Nazim Lakhan, M.; Mehdi, G.; Dong, S. Green synthesis, characterization and photocatalytic application of silver nanoparticles synthesized by various plant extracts., *Arabian Journal of Chemistry*, **2020**, *12*, 1-14, <https://doi.org/10.1016/j.arabjc.2020.01.009>.
13. Lagashetty, A.; Ganiger, S.K. Microwave-Assisted Synthesis, Characterization and Thermal study of Nano sized Metal Aluminates., *J. Met. Mater. Sci.*, **2018**, *60*, 139-148.
14. Taha, A.; Ben Aissa, M.; Da'na, E. Green Synthesis of an Activated Carbon-Supported Ag and ZnO Nanocomposite for Photocatalytic Degradation and Its Antibacterial Activities., *Molecules*, **2020**, *25*, <https://doi.org/10.3390/molecules25071586>.
15. Sharma, D.; Kanchi, S.; Bisetty, K. Biogenic synthesis of nanoparticles: A review. *Arabian Journal of Chemistry* 2019, *12*, 3576-3600, <https://doi.org/10.1016/j.arabjc.2015.11.002>
16. Ulaeto, S.B.; Mathew, G.M.; Pancreicious, J.K.; Nair, J.B.; Rajan, T.P.D.; Maiti, K.K.; Pai, B.C. Biogenic Ag Nanoparticles from Neem Extract: Their Structural Evaluation and Antimicrobial Effects against *Pseudomonas nitroreducens* and *Aspergillus unguis* (NII 08123)., *ACS Biomaterials Science & Engineering*, **2020**, *6*, 235245, <https://doi.org/10.1021/acsbiomaterials.9b0125>.
17. Alenazi, B.; Alsalme, A.; Alshammari, S.G.; Khan, R.A.; Siddiqui, M.R.H. Ionothermal Synthesis of Metal Oxide-Based Nanocatalysts and Their Application towards the Oxidative Desulfurization of Dibenzothiophene., *Journal of Chemistry*, **2020**, *2020*, 21-28, <https://doi.org/10.1155/2020/3894804>.
18. Unuofin, J.O.; Oladipo, A.O.; Msagati, T.A.M.; Lebelo, S.L.; Meddows-Taylor, S.; More, G.K. Novel silverplatinum bimetallic nanoalloy synthesized from Vernonia mespilifolia extract: antioxidant, antimicrobial, and cytotoxic activities., *Arabian Journal of Chemistry*, **2020**, <https://doi.org/10.1016/j.arabjc.2020.06.019>.
19. Sharma, C.; Ansari, S.; Ansari, M.S.; Satsangee, S.P.; Srivastava, M.M. Single-step green route synthesis of Au/Ag bimetallic nanoparticles using clove buds extract: Enhancement in antioxidant bio-efficacy and catalytic activity., *Materials Science and Engineering: C*, **2020**, *116*, <https://doi.org/10.1016/j.msec.2020.111153>.
20. Jana, A.; Scheer, E.; Polarz, S. Synthesis of graphene-transition metal oxide hybrid nanoparticles and their application in various fields., *Beilstein J Nanotechnol.*, **2017**, *8*, 688-714, <https://doi.org/10.3762/bjnano.8.74>.
21. Lagashetty, A.; Patil, M.K.; Ganiger, S.K. Green Synthesis, Characterization, and Thermal Study of Silver Nanoparticles by *Achras sapota*, *Psidium guajava*, and *Azadirachta indica* Plant Extracts., *Plasmonics*, **2019**, *14*, 1219-1226, <https://doi.org/10.1007/s11468-019-00910-3>.
22. Arunkumar Lagashetty.; Sangappa K. Ganiger.; Shashidhar. Synthesis Characterization and antibacterial study of Ag–Au Bi-metallic nanocomposite by bioreduction using piper betle leaf extract., *Heliyon*, **2019**, *5*, e02794, <https://doi.org/10.1016/j.heliyon>.
23. Taha, A.; Ben Aissa, M.; Da'na, E. Green Synthesis of an Activated Carbon-Supported Ag and ZnO Nanocomposite for Photocatalytic Degradation and Its Antibacterial Activities., *Molecules*, **2020**, *25*, <https://doi.org/10.3390/molecules25071586>.
24. Ahirwar, R.C.; Mehra, S.; Reddy, S.M.; Alshamsi, H.A.; Kadhem, A.A.; Karmankar, S.B.; Sharma, A.; Poushali. Progression of Quantum Dots Confined Polymeric Systems for Sensorics. *Polymers*, **2023**, *15*, 405. <https://doi.org/10.3390/polym15020405>.
25. Singh, A.; Ahirwar, R. C.; Borgaonkar, K.; Gupta, N.; Ahsan, M.; Rathore, J., & Rawat, R. Synthesis of Transition-Metal-Doped Nanocatalysts with Antibacterial Capabilities Using a Complementary Green Method., *Molecules*, **2023**, *28*(10), 4182.